U.S. Department of Veterans Affairs
Public Access Author manuscript
Gene Ther. Author manuscript; available in PMC 2016 December 01.

Published in final edited form as:
Gene Ther. 2016 June ; 23(6): 500–509. doi:10.1038/gt.2016.21.

Opposing Effects of Sca-1+ Cell-Based Systemic FGF-2 Gene Transfer Strategy on Lumbar versus Caudal Vertebrae in the Mouse

K.-H. William Lau[1], **Shin-Tai Chen**[1], **Xiaoguang Wang**[1], **Subburaman Mohan**[1], **Jon E. Wergedal**[1], **Chandrasekhar Kesavan**[1], **Apruva K. Srivastava**[2], **Daila S. Gridley**[3], and **Susan L. Hall**[1]

[1]Musculoskeletal Disease Center, Jerry L. Pettis Memorial VA Medical Center, Loma Linda, CA, U.S.A.

[2]Laboratory of Human Toxicology, Pharmacology, Applied/Developmental Research Directorate, SAIC-Frederick, Frederick National Laboratory for Cancer Research, Frederick, MD, U.S.A.

[3]Department of Radiation Medicine, Loma Linda University School of Medicine, Loma Linda, CA, U.S.A.

Abstract

Our previous work showed that a Sca-1$^+$ cell-based *FGF2* therapy was capable of promoting robust increases in trabecular bone formation and connectivity on the endosteum of long bones. Past work reported that administration of FGF2 protein promoted bone formation in red marrow but not in yellow marrow. The issue as to whether the Sca-1$^+$ cell-based *FGF2* therapy is effective in yellow marrow is highly relevant to its clinical potential for osteoporosis, as most red marrows in a person of an advanced age, are converted to yellow marrows. Accordingly, this study sought to compare the osteogenic effects of this stem cell-based *FGF2* therapy on red marrow-filled lumbar vertebrae with those on yellow marrow-filled caudal vertebrae of young adult W^{41}/W^{41} mice. The Sca-1$^+$ cell-based *FGF2* therapy drastically increased trabecular bone formation in lumbar vertebrae, but the therapy not only did not promote bone formation but instead caused substantial loss of trabecular bone in caudal vertebrae. The lack of an osteogenic response was not due to insufficient engraftment of FGF2-expressing Sca-1$^+$ cells or inadequate FGF2 expression in caudal vertebrae. Previous studies have demonstrated that recipient mice of this stem cell-based FGF2 therapy developed secondary hyperparathyroidism and increased bone resorption. Thus, the loss of bone mass in caudal vertebrae might in part be due to an increase in resorption without a corresponding increase in bone formation. In conclusion, the Sca-1$^+$ cell-based FGF2 therapy is osteogenic in red marrow but not in yellow marrow.

*Corresponding author: Susan L. Hall, M.D., Ph.D., Musculoskeletal Disease Center (151), Jerry L. Pettis Memorial VA Medical Center, 11201 Benton Street, Loma Linda, CA 92357, Tel: (909) 825-3084 x 1990, Fax: (909) 796-1680, ; Email: Susan.Hall1@va.gov

Conflict-of-Interest: There is no conflict-of-interest to disclose.

Keywords

FGF2; hematopoietic stem cells; gene therapy; trabecular bone; red marrow; yellow marrow; lumbar vertebrae; caudal vertebrae

Introduction

Osteoporosis is a systemic bone disease of low bone mass associated with impaired bone architecture, characterized by disruption of trabecular continuity through trabecular perforation that results in reduced connectivity of the bone structure and conversion of the normal plate-like trabeculae into thinner rod-like structures.[1] It is resulted from insufficient bone formation to compensate for increases in bone resorption. Most current FDA-approved therapies for osteoporosis, such as, bisphosphonates, selective estrogen receptor modulators, and RANKL inhibitory monoclonal antibody (Denosumab), aim to suppress bone resorption and have demonstrated clinical efficacy.[2] Due to the relatively low bone regenerative capacity of these anti-resorptive drugs (as reflected by only very modest increases in bone density), they are generally inadequate for patients with severe osteoporosis, who have large bone deficits. The acquisition rate of new bone formation achieved with the only FDA-approved anabolic therapy [teriparatide (PTH) injection therapy] may also be insufficient for patients with the highest fracture risk. Patients with severe bone deficits require a potent osteogenic therapy capable of regenerating large amounts of structurally and mechanically sound new bone within a realistic timeframe. Accordingly, there is still unmet demand for a potent osteogenic therapy, especially for patients with severe bone deficits.

Our laboratory has been interested in developing a systemic osteogenic growth factor gene transfer-based therapy for osteoporotic patients with large bone deficits. Our approach was to take advantage of the propensity of hematopoietic stem cells (HSCs) to home to and engraft in the HSC niches within bone marrow cavities,[3] and to develop a HSC-enriched stem cell antigen-1 positive (Sca-1^+) cell-based *ex vivo* gene transfer strategy[4]. This strategy used genetically engineered Sca-1^+ cells to deliver a bone growth factor to the endosteum to promote endosteal bone formation. Our decision of utilizing the fibroblast growth factor (*FGF*)-2 transgene was based on findings that disruption of the *Fgf2* gene in mice reduces bone formation and impairs fracture repair[5,6] and that FGF2 is a potent osteogenic factor capable of stimulating endochondral bone formation in both young and aged ovariectomized (OVX) rats.[7–11] Accordingly, systemic administration of recombinant FGF2 protein promotes rapid bone formation, and increases trabecular bone mass on the endosteal surface without significant effects on periosteal bone formation in OVX rats.[5,12–15] FGF2 also appears to be required for the anabolic action of PTH in bone.[16]

Our recent studies have provided compelling proof-of-concept evidence for the feasibility of this systemic stem cell-based *FGF2* gene transfer strategy.[17,18] Specifically, a single transplantation of genetically modified Sca-1^+ cells expressing a human *FGF2* gene into sub-lethally-irradiated recipient mice yielded robust *de novo* trabecular bone formation and increased trabecular connectivity on the endosteum of long bones.[17,18] While this systemic gene transfer strategy delivering a *FGF2* gene showed huge bone formation-promoting

capacity,[17] employing the same strategy but delivering the bone morphogenic protein-4 (*BMP4*) gene only resulted in modest gains in bone mass,[19] and the use of the human growth hormone (*hGH*) gene even led to significant bone loss.[20] This stem cell-based *FGF2* strategy also increased bone resorption and caused osteomalacia, which presumably was due to secondary hyperparathyroidism developed in response to hypocalcemia that was a consequence of a high circulating level of FGF2 and too rapid of bone formation.[17] However, these adverse effects can be avoided with the use of β-globin promoter to drive *FGF2* to confine FGF2 expression to the bone marrow cavity.[18]

Although other investigators have previously used FGF2 protein therapy to promote endosteal bone formation and had produced very encouraging results,[8,12,13,21–23] our HSC-based *FGF2* gene transfer strategy is novel with respect to the innovative use of HSCs as the cell vehicle for FGF2, which allows targeted FGF2 expression specifically at the stem cell niches along the endosteum. Although direct comparison of the efficacy of the FGF2 protein therapy with that of our stem cell-based strategy is difficult owning to differences in animal models, experimental designs, and treatment duration, our strategy appeared to be >10-times more potent than the protein-based therapy[12,23] in increasing the percentage of trabecular bone area on the endosteum and in increasing trabecular bone parameters. Furthermore, because the administered FGF2 protein is readily metabolized and cleared from the circulation, multiple (daily) injections of the FGF2 protein are required for the protein therapy to produce a detectable biological effect. This requires large supplies of the FGF2 protein, which would be a significant limiting factor. In contrast, the engrafted genetically modified stem cells in our strategy continuously produce FGF2 at the endosteal niches to promote robust endosteal/trabecular bone formation, making multiple administrations of the therapy unnecessary. The combination of these unique and potent regenerative properties renders this systemic stem cell-based *FGF2* gene transfer strategy potentially a more attractive regenerative therapeutic option than the FGF2 protein therapy for treatment of osteoporotic patients with severe bone deficits.

Previous work on the FGF2 protein therapy of Wronski and coworkers, however, has also disclosed an intriguing observation in that the osteogenic effect of the FGF2 protein therapy seen in red marrow skeletal sites (proximal femurs and lumbar vertebrae) was greatly attenuated in skeletal sites containing largely yellow marrows (distal tibia and caudal vertebrae).[24,25] Since almost all of the bone marrows in a person of an advanced age is converted to yellow marrows,[26] and since osteoporosis is largely an aging disorder and patients with severe osteoporosis are usually the elderly, our stem cell-based *FGF2* gene transfer strategy must also be able to promote bone formation in yellow marrow cavities in order for it to be useful in treating elderly osteoporotic patients. Accordingly, the issue as to whether our strategy is also effective in yellow marrow sites is highly relevant to its clinical potential. Consequently, our primary goal for the present study was to determine if our Sca-1^+ cell-based *FGF2* gene transfer strategy is as efficacious in the yellow marrow-containing caudal vertebrae as in the red marrow-containing lumbar vertebrae.

Results

Marrow transplantation of Sca-1$^+$ cells expressing *FGF2* increased circulating and local FGF2 levels in recipient mice

To assess whether our systemic Sca-1$^+$ cell-based *FGF2* gene transfer strategy would promote trabecular bone formation in lumbar vertebrae, we transplanted W^{41}/W^{41} recipient mice with MLV-*gfp*-transduced or MLV-*FGF2*-transduced Sca-1$^+$ cells (n = 7 per group). Engraftment of donor cells, which was assessed by measuring the relative percentage of peripheral *gfp*-expressing blood cells at 6 weeks post-transplantation, was ~70% (data not shown). To confirm an effective engraftment of MLV-*FGF2*-transduced Sca-1$^+$ cells in recipient mice, we measured the relative levels of *FGF2* genomic DNA in extracts of peripheral blood cells of recipient mice by real-time PCR, using a primer set that is specific for the human *FGF2* transgene and that does not recognize the endogenous murine *Fgf2* gene of the host. The human *FGF-2* DNA content in recipient mice of MLV-*FGF2*-transduced Sca-1$^+$ cells at both 6 and 14 weeks post-transplantation was each ~600-fold greater than that in recipient mice of MLV-*gfp*-transduced Sca-1$^+$ cells recipient control mice (Fig. 1A). The serum level of FGF-2 protein in recipient mice of MLV-*FGF2*-transduced cells was also 15-fold greater than that in the control group at 14 weeks post-transplantation (Fig. 1B). These findings confirm an effective and relatively stable engraftment of the donor *FGF2*-expressing Sca-1$^+$ cells in recipient mice.

Our previous studies showed that marrow transplantation of FGF-2-expressing Sca-1$^+$ cells not only promoted robust endosteal/trabecular bone formation, but also caused secondary hyperparathyroidism due to hypocalcemia developed in response to the rapid increase in bone formation.[24] Consistent with the previous findings, Fig. 1C shows that the serum PTH level of recipient mice of MLV-*FGF2*-transduced Sca-1$^+$ cells at 14 weeks post-transplantation was more than 10-fold that in control mice receiving MLV-*gfp*-transduced Sca-1$^+$ cells (>100 pg/mL in *FGF2* mice vs. 9.8 ± 0.8 pg/mL in *gfp* control mice). Serum PTH level in the *gfp*-treated control mice was not significantly different from that of untreated control mice (10.7 ± 0.6 pg/mL), indicating that the increase in serum PTH was in response to *FGF2* transgene expression and not to Sca-1$^+$ cell transplantation *per se*.

Sca-1$^+$ cell-based *FGF2* gene therapy promoted robust bone formation but caused osteomalacia in lumbar vertebrae

The robust enhancing effects of the Sca-1$^+$ cell-based *FGF2* gene transfer strategy on endosteal/trabecular bone formation in femurs of recipient mice have been reported previously.[17] To determine whether this *FGF2* gene therapy would also similarly promote *de novo* trabecular bone formation in lumbar vertebrae, cross-sections of L3 vertebrae of recipient mice of Sca-1$^+$ cells transduced with MLV-*FGF2* and those of recipient mice of MLV-*gfp*-transduced Sca-1$^+$ cells were stained with Goldner's trichrome dye for mineralized bone matrices. Fig. 2 shows dramatic histologic changes in vertebrae of mice with high expression levels of *FGF2* (right panel) compared to *gfp* control mice (left panel). There were large increases in newly formed bone matrix areas that nearly filled the entire marrow cavity of recipient mice of the *FGF2* group. However, a large majority of these newly formed matrix areas were un- or under-mineralized (stained red). Nevertheless, the osteoid

layers exhibited a matrix pattern similar to newly laid lamellar bone and not woven bone. The pattern of wide layers of un- or under-mineralized lamellar bone in the *FGF2* group suggests that the gene transfer strategy caused similar robust increases in trabecular bone formation in lumbar vertebrae as that seen in long bones.[17,18] Also, similar to MLV-*FGF2*-treated femurs,[17] the under-mineralization of the newly formed trabecular bones is presumably the consequence of the hypocalcemia and secondary hyperparathyroidism developed in recipient mice with too high of a level of rapid bone formation.[17]

We next measured quantitative static bone histomorphometry parameters on the L3 vertebra. The results were averaged over six consecutive microscopic fields, at 10× magnification, beginning from a point 350 μm distal from the inferior edge of the bone growth plate. As shown in Fig. 3, the % osteoid area (%O.Ar) (increased 4.6-fold), % forming surface (%L.Pm) (increased 1.9-fold) and trabecular width (Tb.Wi) (increased 1.3-fold) in L3 vertebrae of recipient mice transplanted with MLV-*FGF2*-transduced Sca-1$^+$ cells were each significantly increased compared to those in the *gfp* control recipient mice. Conversely, the % mineralized bone area (%Md.Ar) was significantly decreased (by 27%) in the *FGF2*-transplanted group compared to the *gfp* control group. The trabecular number (Tb.N) was not different between the two groups. These quantitative histomorphometry measurements of L3 vertebra were compatible with the microscopic bone changes that show a pattern of large increases in new bone formation but with significant reduction in the amounts of mineralized bone (Fig. 2). These findings indicate that the Sca-1$^+$ cells-based *FGF2* gene therapy led to similar robust trabecular bone formation in lumbar vertebrae as seen in long bones.[17,18] Similar to those in the *FGF2* gene therapy-treated femurs, the large amounts of largely un- or under-mineralized newly formed bone in lumbar vertebrae are presumably also the result of the hypocalcemia and secondary hyperparathyroidism developed in response to excessively high levels of FGF2 expression and too rapid of an increase in bone formation.[17]

Transplantation of MLV-*FGF2*-transduced Sca-1$^+$ cells in mice led to substantial loss of trabecular bone mass in caudal vertebrae

To examine the possibility that donor FGF2-expressing Sca-1$^+$ cells might target the highly vascularized red marrow skeletal sites rather than the poorly vascularized yellow marrow sites for engraftment, we performed a second transplantation experiment to compare osteogenic effects of the Sca-1$^+$-based *FGF2* gene therapy on the proximal femur metaphysis (a red marrow skeletal site) with that on the caudal vertebra (a yellow marrow skeletal site). In this experiment, W^{41}/W^{41} recipient mice were transplanted with 500,000 MLV-*gfp*-transduced or MLV-*FGF2*-transduced Sca-1$^+$ cells. We first measured levels of serum FGF-2, serum and tibial extract ALP activity, and serum PTH of each recipient mouse at 14 weeks post-transplantation to ensure successful transplantation. Consistent with our previous findings, recipient mice transplanted with MLV-*FGF2*-transduced Sca-1$^+$ cells showed ~4,000-fold increase in serum FGF2 (Fig. 4A) and ~8-fold increase in serum PTH (Fig. 4B) compared to control recipient mice transplanted with MLV-*gfp*-transduced Sca-1$^+$ cells. The *FGF2* group of mice also exhibited elevated serum (Fig. 4C) and bone (Fig. 4D) ALP levels (a biomarker of bone formation).

We next performed μ-CT analysis on the metaphysis of femur and on the S3 caudal vertebra of each recipient mouse. Top panels of Fig. 5A shows the μ-CT three-dimensional reconstruction of the femur metaphysis of a representative recipient mouse transplanted either with MLV-*gfp*-transduced Sca-1$^+$ cells or with MLV-*FGF2*-transduced cells. As expected, *FGF2* gene therapy yielded large increases in trabecular bone volume (Tb.BV/TV) and thickness (Tb.Th), without altering trabecular number (Tb.N) or separation (Tb.Sp) at the femur metaphysis (Fig. 5A, bottom panels). Conversely, transplantation of MLV-*FGF2*-transduced Sca-1$^+$ cells not only did not yield robust increases in trabecular bone mass in the S3 caudal vertebra, but in fact led to substantial reduction in trabecular bone mass compared to control mice (Fig. 5B). The findings of the ~40% reduction in Tb.N, the approximately two-fold increase in Tb.Sp., along with no significant changes in Tb.Th, are consistent with an increase in bone resorption in caudal vertebra (Fig. 5B, bottom panel). Consequently, it appears that the absence of an increase in bone formation, along with the apparent increase in bone resorption, resulted in substantial loss of trabecular bone mass in the caudal vertebra.

Sca-1$^+$ cell-based *FGF2* gene therapy-associated trabecular bone loss in caudal vertebrae was not due to insufficient local FGF2 production

To determine whether the lack of an anabolic response in caudal vertebrae of recipient mice was caused in part by inefficient engraftment of donor Sca-1$^+$ cells at yellow marrow skeletal sites, we performed a third marrow transplantation experiment, in which we compared the relative engraftment efficiency of 500,000 donor Sca-1$^+$ cells isolated from TgN-GFP transgenic mice, transduced with MLV-*FGF2* (test group) or MLV-*β-gal* (control group), in the marrow cavity of femurs at 6 weeks post-transplantation with that in the marrow cavity of S3 caudal vertebrae of recipient mice. To assess engraftment efficiency, bone marrow cells were flushed out of femurs of each recipient mouse. Total RNA of marrow cells was isolated and reverse-transcribed to cDNA and the relative *gfp* mRNA level (as an index of engraftment of donor cells) was determined by real-time PCR. Because marrow cells of caudal vertebrae could not be flushed out easily, we opted to isolate total RNA from the entire caudal vertebra. Thus, the caudal vertebrae RNA samples differed from the femur marrow cell RNA samples, in that the caudal vertebra samples contained RNAs derived from both bone marrow cells and bone cells. Fig. 6A shows that the *gfp* mRNA levels between recipient mice of MLV-*β-gal*-transduced *gfp* transgenic Sca-1$^+$ and recipient mice of MLV-*FGF2*-transduced *gfp* transgenic Sca-1$^+$ cells did not differ statistically from each other at the S3 caudal vertebra or at the femur. On the other hand, comparison of the relative *gfp* mRNA expression level between the two bone sites of the FGF2 group of mice alone (without normalizing against each respective MLV-*β-gal* control) showed that *gfp* mRNA expression was significantly higher in bone marrow cells of femurs than in bone extracts of S3 caudal vertebra ($P<0.0002$) (Fig. 6B). However, because the caudal vertebra samples contained RNA derived not only from marrow cells but also from vertebral bone, the possibility that the different amounts of *gfp* mRNA detected in femur bone marrow cells (as opposed to that in caudal vertebra) may be due to the different cellular sources of RNA from the two skeletal sites cannot be ruled out.

To further evaluate the possibility that the lack of an osteogenic response in caudal vertebrae of recipient mice transplanted with *FGF2*-expressing Sca-1$^+$ cells was caused by an inefficient expression of *FGF2* at yellow marrow sites, we compared the relative fold-increases in the *FGF2* mRNA level in bone marrow cells of the femur with that in S3 caudal vertebra by real-time RT-PCR. As expected, *FGF2* expression at the femur and caudal vertebra was significantly higher in the *FGF2* group of mice compared to *β-gal* control group of mice at both skeletal sites (i.e., 1024-fold, $p<0.0001$ for femur, 1830-fold, $p<0.001$ for caudal vertebra). (Fig. 7) However, there was no significant difference between *FGF2* mRNA expression in the femur site and that in caudal vertebra site in either *FGF2* mice or *β-gal* control mice. These findings strongly suggest that the trabecular bone loss in caudal vertebrae was not caused by an inefficient expression of *FGF2* in caudal vertebrae.

Discussion

In this study, we confirmed that our stem cell-based *FGF2* gene transfer strategy is highly effective in promoting trabecular bone formation at the endosteal surface throughout the marrow cavity of femurs.[17,18] It also provided compelling evidence that this strategy is highly osteogenic in the lumbar vertebra. This conclusion is based on the findings of large increases in un-mineralized bone area (Fig. 2), %O.Ar (Fig. 3), and mineralized bone mass [as evidenced by the increase in Tb.BV/TV (data not shown)], as well as large increases in % forming surface (%L.Pm) and trabecular width (Tb.Wi) in lumbar vertebrae of FGF-2-treated mice compared to control mice. The findings that this therapeutic approach is capable of promoting robust trabecular bone formation and regeneration of trabecular structure in both proximal femurs and lumbar vertebrae could have clinical implication, since the lumbar spine and the hip are two of the most common skeletal sites for non-traumatic osteoporotic fractures.

Previous studies reported that the FGF2 protein therapy was unable to promote bone formation in skeletal sites with yellow marrows, such as the caudal vertebrae.[24,25] The FGF2 protein therapy strategy differs from our strategy in many aspects, such as differences in tissue-targeting mechanisms, delivery kinetics, achievable local FGF2 concentrations, and metabolism clearance rates. Unlike red marrows, which are highly vascularized, there is very little vascular structure in yellow marrows. This reduced vascular network may limit the accessibility of the systemically administered FGF2 protein in yellow marrow cavities. In contrast, FGF2-expressing Sca-1$^+$ cells engraft at HSC niches, presumably in both red and yellow marrows, and produce FGF2 continuously at local sites, resulting in relatively high local FGF2 levels. To our surprise, we also found that, similar to the FGF2 protein therapy,[24,25] our stem cell-based therapy also did not yield significant increase in trabecular bone formation in caudal vertebrae. More surprisingly and contrary to the findings of the FGF2 protein therapy that did not result in any bone loss in caudal vertebrae,[24,25] our therapy in fact caused substantial trabecular bone loss in caudal vertebrae, as reflected by >40% reduction in Tb.BV/TV and Tb.N (Fig. 5).

The mechanistic reason for the apparent lack of an osteogenic action of the two FGF2-based therapies in yellow marrow-filled caudal vertebrae is not well understood. Previous studies have suggested that the lack of an osteogenic response to FGF2 in caudal vertebrae was not

due to an insufficient expression of the FGF2 receptors, since there was no significant difference in expression levels of the various surface FGF2 receptors between cells on the endosteal surface of red marrow sites compared to that of yellow marrow in caudal vertebrae.[24] Similarly, the lack of an osteogenic effect of our stem cell-based systemic FGF2 gene therapy was also not due to inadequate expression of the FGF2 transgene locally, since we found no significant differences in the relative engraftment efficiency of the transplanted GFP-expressing Sca-1^+ cells in femurs from that in caudal vertebrae of recipient mice (Fig. 6), and since marrow transplantation of FGF2-expressing Sca-1^+ cells yielded >1,000-fold increase in the local *FGF2* mRNA level in both femurs and in caudal vertebrae (Fig. 7). A major difference between the two types of vertebrae is that lumbar vertebrae contain largely red marrow with some amounts of adipose tissues; but caudal vertebrae is made up of predominantly yellow marrow, which is filled largely with adipocytes,[24] thus raising the possibility that the site-specific differences in the skeletal response to the FGF2 treatment could be in part due to differences in the cellular composition between red and yellow marrows. In this regard, mesenchymal stem cells (MSCs) are more abundant in red marrow than in yellow marrow. Multipotent MSCs can be committed into progenitor cells of osteogenic, chondrogenic, or adipogenic lineages, depending on the type of cellular signals released from the local milieu.[27] FGF2 stimulates osteoblastic differentiation of MSCs and osteoblastic bone formation.[5,28–31] In red marrow sites, MSCs favor the osteogenic (or chondrogenic) lineage; whereas MSCs in yellow marrow tend to commit to the adipocytic lineage. As a result, there may be limited numbers of MSCs committed to the osteoblastic lineage in yellow marrows when compared to red marrows, thus greatly reducing the osteogenic response to FGF2. The difference in response to FGF2 therapies between lumbar and caudal vertebra could also be due, at least in part, to differences in weight bearing at the two sites. These are interesting possibilities, some of which will be evaluated in our future studies.

The mechanistic cause for the substantial loss of trabecular bone mass in caudal vertebrae of the recipient mice of the FGF2-expressing Sca-1^+ cells is unknown at this time. FGF2 has been shown to promote osteoclastogenesis and bone resorption *in vitro*.[32–36] Our findings of ~40% reduction in Tb.N and ~two-fold increase in Tb.Sp., along with no significant changes in Tb.Th (Fig. 5B, bottom panel) in caudal vertebrae of mice treated with the FGF2 gene therapy, are consistent with an increase in bone resorption at this skeletal site. Thus, it is possible that the trabecular bone loss is due to an increase in bone resorption without a corresponding increase in bone formation. In addition, the effects of adipocytes (and their secretory factors) on osteoclastogenesis are complex,[37] as both positive and negative effects on the survival and actions of osteoclasts and precursors have been reported. Therefore, we cannot rule out the possibility that the increased bone resorption in yellow marrows could be due to their increased lipid content. We should emphasize that recipient mice transplanted with *FGF2*-transduced Sca-1^+ cells, especially those with high circulating levels of FGF2, developed hypocalcemia, secondary hyperparathyroidism, and osteomalacia (Fig. 1 and 4). Secondary hyperparathyroidism is a well-known pathologic cause of increased resorption. Therefore, inasmuch as it is possible that direct activation of osteoclastogenesis by high concentrations of local FGF2 could play a contributing role in the observed increase in bone resorption, the primary contributing factor is most likely secondary hyperparathyroidism,

which presumably developed in response to the large and too rapid increase in bone formation.[20] In support of this tentative conclusion, the FGF2 protein therapy, which did not induce hypocalcemia or secondary hyperparathyroidism, did not increase bone resorption in bone sites in yellow marrows.[24,25] We have recently modified our stem cell-based *FGF2* therapy to use the erythroid promoter to confine FGF2 expression to the marrow cavity, and found that this modification was effective and also avoided development of hypocalcemia, secondary hyperparathyroidism, and osteomalacia.[18] Therefore, we will in the future determine whether the prevention of secondary hyperparathyroidism with the use of the erythroid promoter could prevent the increase in bone resorption and the bone loss in caudal vertebrae.

On the basis of our findings, we have advanced a model (Fig. 8) that may account for the contrasting effects of the stem cell-based *FGF2* therapy on red marrows as opposed to yellow marrows. In this model, we envision that our strategy leads to sustained elevation of local levels of FGF2 in both red and yellow marrows. We postulate that there are large numbers of uncommitted MSCs and osteoprogenitors in red marrows (left side of Fig. 8), where FGF2 acts on uncommitted MSCs and osteoprogenitors to promote osteoblastic differentiation. This leads to robust and rapid increases in endosteal/trabecular bone formation in red marrows. We further speculate that there is insufficient dietary calcium to meet the huge demand for calcium needed for the rapid and massive increase in bone formation. As a consequence, hypocalcemia and secondary hyperparathyroidism develop, which in turn increases bone resorption at both red and yellow marrows. Because the increase in bone formation is larger than that of bone resorption in red marrows, the result is a net increase in bone mass. Conversely, there are very limited numbers of uncommitted MSCs and osteoprogenitors in yellow marrows (right side of Fig. 8) for FGF2 to act on. Accordingly, the elevated FGF2 levels have little or no osteogenic effects. This lack of a significant bone formation at the yellow marrows, coupled with the increased resorption rate related to hyperparathyroidism, leads to substantial loss of trabecular bone mass in yellow marrows.

In conclusion, this study highlights an important issue that is highly relevant to the clinical potential of our stem cell-based FGF2 gene transfer therapy for severe osteoporosis. While our strategy is capable of promoting endosteal/trabecular bone formation in proximal femurs as well as lumbar vertebrae, it lacks osteogenic effects in yellow marrows. This inability to promote regeneration of trabecular bone structure in yellow marrow skeletal sites would greatly reduce the clinical utility of this strategy, and must be overcome before it can be used to treat patients with severe bone deficits. Our future understanding of how and why FGF2 promotes trabecular bone formation in red but not yellow marrows would provide insights as to how to improve on the efficacy of the therapy in yellow marrows. Consequently, our future work will focus on the mechanistic aspects of this therapy in order to improve on its clinical potential.

Materials and Methods

Animals

C57BL/6J mice were purchased from the Jackson Laboratories (Bar Harbor, ME, USA). Trans-Golgi network β-actin-enhanced green fluorescent protein (TgN-GFP) transgenic mice (in C57BL/6J genetic background) were also purchased from the Jackson Laboratories. The W^{41}/W^{41} mutant strain of mice (in C57BL/6J genetic background) [originally provided by Dr. Jane Barker of the St Louis University School of Medicine (St. Louis, MO, USA)] was used as transplantation recipients in all transplantation experiments. This mouse strain was used as recipient mice, because, as a result of a point mutation in the c-kit gene,[38] they are deficient in the number of hematopoietic stem cells[39] and thereby require significantly lower levels of irradiation than WT mice for highly efficient engraftment during the bone marrow transplantation procedure.[40] The femoral BMD of female (but not male) W^{41}/W^{41} mice was 17% lower than that of age-matched female WT littermates.[41] However, because total body irradiation is known to cause significant bone loss and it has been well-recognized as a major etiologic factor for osteoporosis in bone marrow transplantation,[42] this mouse model may be considered as an animal model of radiation-induced osteoporosis. Animals were housed within the Veterinary Medical Unit of the Loma Linda Veterans Affairs Healthcare System. All animal procedures were reviewed and approved by two Institutional Animal Care and Use Committees (Loma Linda Veterans Affairs Healthcare System and Loma Linda University).

Bone marrow Sca-1$^+$ cell population isolation

Detailed description of methods for Sca-1^+ cell harvest and isolation are previously described elsewhere.[17] Briefly, whole bone marrow (WBM) cells were harvested from donor mice by flushing tibiae and femurs with phosphate-buffered saline (PBS) plus 0.5% bovine serum albumin (Sigma-Aldrich, St. Louis, MO) using a needle and syringe. Erythrocytes were removed by osmotic lysis and the remaining mononuclear cell preparation was enriched for Sca-1^+ cells by passage twice through an automatic magnetic assisted cell separation column (AutoMacs®), after incubation with magnetic microbeads conjugated with antibody specific for Sca-1 (Miltenyi Biotec, Inc., Auburn, CA, USA) according to manufacturer's instructions. To assess enrichment effectiveness, aliquots of each cell fraction were incubated with phycoerythrin (PE)-conjugated Sca-1-specific or PE-conjugated rat isotype control antibody (Pharmingen, San Diego, CA, USA) and analyzed for Sca-1 and/or GFP-expression by fluorescence activated cell sorter (FACS) analysis with a FACSCalibur or FACSAria System (BD Biosciences, San Jose, CA, USA). The percentage of Sca-1^+ cells was calculated by subtracting the value obtained with the PE-conjugated isotype control antibody from that obtained with the PE-conjugated Sca-1-specific antibody. Similar to previous work,[4,17] approximately 70% of the cells in the isolate after the enrichment expressed the Sca-1 marker.

MLV-based human FGF-2 expression vectors

The generation of MLV-based vectors expressing the enhanced *GFP* marker or a modified human *FGF2* gene has been described in detail elsewhere.[17] To increase secretion efficiency and stability of the expressed FGF2 recombinant protein, the human *FGF2* gene was

modified by adding the BMP2/4 hybrid secretion signaling sequence to its N-terminus and mutating two key cysteines (cys-70 and cys-88) to serine and aspartitic acid, respectively.[43] The MLV-*β-galactosidase* (*β-gal*) was generated as described in detail elsewhere.[44]

Transduction of Sca-1$^+$ cells with MLV-based vectors

Briefly, Sca-1$^+$ cells were plated in 6-well plates (Becton Dickinson, Franklin Lakes, NJ) coated with retronectin (Takara, Otsu, Shiga, Japan) at a density of 4×10^6 cells/well in Iscove's modified Dulbecco's medium (Invitrogen, Grand Island, NY) containing 20% fetal bovine serum (BioWhitaker, Walkersville, MD), 50 ng/mL of human flt-3L, 50 ng/mL of murine stem cell factor, 50 ng/mL of interleukin-6, 10 ng/mL of murine interleukin-3, 0.1 ng/mL murine interleukin-1α (all from Peprotech, Rocky Hills, NJ), 100 μmol/L of deoxyribonucleotide triphosphate (Roche Diagnostics, Indianapolis, ID), as described previously.[17] After overnight incubation, 40 μL of MLV-*gfp*, MLV-*FGF2* or MLV-*β-galactosidase* (*β-gal*) concentrated viral stock (5×10^5 transforming units/μL) was applied to the cells. The medium was removed 8 hours later, and the transduction was repeated once. Cell yields were measured by manual count of viable cells as determined by trypan dye exclusion, and transduced cells were transplanted into recipient mice 20 hours after transduction.

Marrow transplantation

The Sca-1$^+$ transplantation procedure was performed as described previously[17]. Two weeks before and two weeks after irradiation, recipient mice were provided sterile food and autoclaved, acidified water (pH 2.0–2.5) containing 50 mg/L neomycin sulfate (Sigma-Aldrich, St. Louis, MO) and 13 mg/L polymixin B sulfate (Sigma-Aldrich, St. Louis, MO). Mice were preconditioned by total body irradiation from a ^{60}Co source delivering a single irradiation dose of 5 Gy (80 cGy/minute). Each transduced donor Sca-1$^+$ cells were then transplanted into anesthetized recipient mice 4 hours after irradiation via retro-orbital injection.

Three marrow transplantation experiments were performed. In the first experiment, fourteen W^{41}/W^{41} mice were transplanted with 850,000 (in 30 μL sterile saline) Sca-1$^+$-enriched cells transduced with MLV-*gfp* or MLV-*FGF2* viral vector (N=7 per group). Donor Sca-1$^+$ cells were isolated from wild-type (WT) C57BL/6J mice. At 6 weeks and 14 weeks post transplantation, transduction and engraftment efficiencies were evaluated as a single measurement of *FGF2* DNA levels in the cell extracts of recipient peripheral blood, by real time PCR. Primers specific for the human *FGF2* DNA sequence were used and relative fold changes were calculated by the Livak-Schmittgen Method.[45] In the second transplantation experiment, sixteen W^{41}/W^{41} mice were transplanted with 500,000 (in 30 μL sterile saline) Sca-1$^+$-enriched cells transduced with either MLV-*gfp* or MLV-*FGF2* viral vector (N=8 per group). Four mice died (1 from GFP group and three from FGF2 group) before endpoint. In the third transplantation experiment, we made the following three changes from the second experiment: 1) we used GFP-expressing Sca-1$^+$ cells from TgN-GFP mice as donor cells in the transplantation, so that engraftment of GFP-transgenic Sca-1$^+$ cells could be tracked and assessed; 2) we used MLV-*βgal* rather than the MLV-*gfp* as the control viral vector, since the donor cells already expressed GFP; and 3) because we typically had seen a wide variation in

FGF2 expression in FGF2-transplanted group, and in contrast we had seen consistency in our measurements with control mice, we increased the number of the test group (n = 20), i.e., recipients of MLV-FGF2-transduced Sca-1^+ cells, and slightly reduced the number of recipient mice in the control group (n = 4) that were transplanted with MLV-*βgal*-transduced Sca-1^+ cells.

Serum and bone extract analyses

Serum FGF2 and parathyroid hormone (PTH) levels of recipient mice were determined with respective enzyme-linked immunosorbent assay (ELISA) kits (R&D Systems, Minneapolis, MN and ALPCO, Salem, NH, respectively). Serum alkaline phosphatase (ALP) activity was measured with a Hitachi 912 Clinical Chemistry analyzer (Stratec SA Plus, White Plains, NY). Bone extract ALP activity was determined as previously described.[46] Briefly, tibiae of recipient mice were dissected and extracted with 0.1% Triton X-100 solution for 72 hours. The extracts were then assayed in duplicate for ALP activity by colorimetric assay in 96-well plates in a total volume of 0.3 mL, containing 100 mmol/L Na_2CO_3 buffer (pH 10.3), 10 mmol/L *p*-nitrophenyl phosphate, and 1 mmol/L $MgCl_2$. The time-dependent increase in absorbance at 405 nm (reflecting *p*-nitrophenol production) was determined on a microtiter plate spectrophotometer (Model EAR 400 AT, SLT Lab Instruments, Hillsborough, NC, USA). The ALP activity was calculated as U/L of serum or mU/mg dry weight of bone, where one unit of activity is defined as the production of 1 μmol of *p*-nitrophenol per minute at 22±2 °C.

Static histomorphometry of the vertebrae

At 14 weeks post transplantation, mice were euthanized. Vertebrae T12 to L6 were harvested from recipient mice and the bone was cleared of muscle and other soft tissues as much as possible. The vertebrae were fixed in 10% formalin for 4 hours, and stored in 0.05% sodium azide/phosphate buffered saline solution at 4°C. L2–3 vertebrae were located by anatomical landmark (T12-rib junction). A 0.01 inch diameter hollow metal sleeve surrounding a fine copper wire was inserted into the L2-L3 intravetebral space. After confirmation of correct anatomical placement by Faxitron imaging, the metal sleeve was withdrawn, leaving the wire in place. The L2–L3 bones were then dissected and embedded into methylmethacrylate, and serial thin sections (5 μm in thickness) were then stained with Goldner's trichrome dye for analysis of matrix mineralization.

Micro-computed tomography (μCT)

Three-dimensional bone parameters were assessed on distal femurs or S3 caudal vertebrae by μ-CT using a Scanco vivaCT40 μ-CT scanner (Scanco Medical Brüttisellen, Switzerland) as previously described.[47] Trabecular measurements were performed at the secondary spongiosa of distal femur (at a site that was 10% of the full length of the femur from the distal end) or the entire S3 caudal vertebra. Accordingly, a region of 0.8 mm in thickness at 10% of the full length from the distal end of each femur was scanned. The trabecular masks were defined in a semiautomatic manner, starting from the outer mask of the femur and application of 15 erosion cycles to ensure that no cortex was included in the measurement. The slices were analyzed using the threshold setting of 230–1,000 mg/cm^3. Bone parameters were calculated using the analytical tool software of Scanco.

DNA/RNA extraction and quantitative real-time reverse transcriptase polymerase chain reaction (RT-PCR)

Total DNA was isolated from cells using the Qiagen QIAamp DNA Blood Mini Kit (Qiagen, Valencia, CA, USA), and total RNA was isolated using the Qiagen RNeasy Mini kit. The cDNA of each RNA sample was synthesized with the Superscript II RT first strand synthesis system (Invitrogen, Carlsbad, CA, USA), 250 ng of random hexamer primers and 160 ng of total RNA in a 20-μl volume. Real-time PCR reactions were performed with 2 μl of DNA or cDNA, 10 pmol of each primer set, and HotStarTaq DNA Polymerase using a QuantiTect SYBR Green PCR Kit (Qiagen) in an Opticon DNA Engine (MJ Research/Bio-Rad, Hercules, CA, USA). To normalize the data, a primer set unique to mouse peptidylproplyl isomerase A (*Ppia*) (accession number: NM 008 907.1) [forward (position 314) 5'-GCA TAC AGG TCC TGG CAT CT-3', reverse (position 501) 5'-TGC TGG TCT TGC CAT TC-3'] was used. To distinguish transgenic human *FGF2* mRNA from endogenous murine *Fgf2* mRNA, the *FGF2* primers used for the PCR reaction were specific to the human *FGF2* gene (accession number: NM 002006.4) [forward (position 578) 5'-GGCTTCTTCCTGCGCATCC-3', reverse (position 900) 5'-CAGGACCTGGGCAGAAAGC-3'. Since mice transplanted with cells transduced with the MLV-*βgal* vector do not express the human *FGF2* gene, the critical cycle threshold (CT) value of 38 (the basal 'noise' value of our RT-PCR analysis) was assigned to the specimen of these control mice in order to calculate ΔCT values. Relative mRNA abundances were quantified as the critical cycle threshold (ΔCT) method: CT of the gene-of-interest − CT of housekeeping gene. The results are shown as the mean ± SEM of duplicates, with the difference in one cycle representing a two-fold difference in relative mRNA abundance. Fold changes were calculated by the $2^{-\Delta\Delta CT}$ method[45].

Statistical analysis

Comparisons of differences were performed using two-tailed, two-sample independent *t*-tests. Results were considered significant when $P<0.05$. All data are reported as mean ± SEM.

Acknowledgments

This work was supported in part by a Merit Review Entry Program grant from the Department of Veterans Affair Medical Research program. All work, except the irradiation procedure, was performed in facilities provided by the Department of Veterans Affairs.

References

1. Kalpakcioglu BB, Morshed S, Engelke K, Genant HK. Advanced imaging of bone macrostructure and microstructure in bone fragility and fracture repair. J Bone Joint Surg Am. 2008; 90(Suppl 1): 68–78. [PubMed: 18292360]
2. Iwamoto J, Takeda T, Sato Y. Efficacy and safety of alendronate and risedronate for postmenopausal osteoporosis. Curr Med Res Opin. 2006; 22:919–928. [PubMed: 16709313]
3. Spangrude GJ, Brooks DM, Tumas DB. Long-term repopulation of irradiated mice with limiting numbers of purified hematopoietic stem cells: in vivo expansion of stem cell phenotype but not function. Blood. 1995; 85:1006–1016. [PubMed: 7849289]

4. Hall SL, Lau KH, Chen ST, Felt JC, Gridley DS, Yee JK, et al. An improved mouse Sca-1+ cell-based bone marrow transplantation model for use in gene- and cell-based therapeutic studies. Acta Haematol. 2007; 117:24–33. [PubMed: 17095856]
5. Montero A, Okada Y, Tomita M, Ito M, Tsurukami H, Nakamura T, et al. Disruption of the fibroblast growth factor-2 gene results in decreased bone mass and bone formation. J Clin Invest. 2000; 105:1085–1093. [PubMed: 10772653]
6. Hurley MM, Okada Y, Xiao L, Tanaka Y, Ito M, Okimoto N, et al. Impaired bone anabolic response to parathyroid hormone in Fgf2−/− and Fgf2+/− mice. Biochem Biophys Res Commun. 2006; 341:989–994. [PubMed: 16455048]
7. Mayahara H, Ito T, Nagai H, Miyajima H, Tsukuda R, Taketomi S, et al. In vivo stimulation of endosteal bone formation by basic fibroblast growth factor in rats. Growth Factors. 1993; 9:73–80. [PubMed: 7688520]
8. Liang H, Pun S, Wronski TJ. Bone anabolic effects of basic fibroblast growth factor in ovariectomized rats. Endocrinology. 1999; 140:5780–5788. [PubMed: 10579344]
9. Nakamura K, Kurokawa T, Kawaguchi H, Kato T, Hanada K, Hiyama Y, et al. Stimulation of endosteal bone formation by local intraosseous application of basic fibroblast growth factor in rats. Rev Rhum Engl Ed. 1997; 64:101–105. [PubMed: 9085444]
10. Nakamura K, Kurokawa T, Aoyama I, Hanada K, Tamura M, Kawaguchi H. Stimulation of bone formation by intraosseous injection of basic fibroblast growth factor in ovariectomised rats. Int Orthop. 1998; 22:49–54. [PubMed: 9549582]
11. Wronski TJ, Ratkus AM, Thomsen JS, Vulcan Q, Mosekilde L. Sequential treatment with basic fibroblast growth factor and parathyroid hormone restores lost cancellous bone mass and strength in the proximal tibia of aged ovariectomized rats. J Bone Miner Res. 2001; 16:1399–1407. [PubMed: 11499862]
12. Lane NE, Kumer J, Yao W, Breunig T, Wronski T, Modin G, et al. Basic fibroblast growth factor forms new trabeculae that physically connect with pre-existing trabeculae, and this new bone is maintained with an anti-resorptive agent and enhanced with an anabolic agent in an osteopenic rat model. Osteoporos Int. 2003; 14:374–382. [PubMed: 12768279]
13. Yao W, Hadi T, Jiang Y, Lotz J, Wronski TJ, Lane NE. Basic fibroblast growth factor improves trabecular bone connectivity and bone strength in the lumbar vertebral body of osteopenic rats. Osteoporos Int. 2005; 16:1939–1947. [PubMed: 16086094]
14. Iwaniec UT, Magee KA, Mitova-Caneva NG, Wronski TJ. Bone anabolic effects of subcutaneous treatment with basic fibroblast growth factor alone and in combination with estrogen in osteopenic ovariectomized rats. Bone. 2003; 33:380–386. [PubMed: 13678780]
15. Power RA, Iwaniec UT, Wronski TJ. Changes in gene expression associated with the bone anabolic effects of basic fibroblast growth factor in aged ovariectomized rats. Bone. 2002; 31:143–148. [PubMed: 12110427]
16. Fei Y, Xiao L, Hurley MM. The impaired bone anabolic effect of PTH in the absence of endogenous FGF2 is partially due to reduced ATF4 expression. Biochem Biophys Res Commun. 2011; 412:160–164. [PubMed: 21806973]
17. Hall SL, Lau KH, Chen ST, Wergedal JE, Srivastava A, Klamut H, et al. Sca-1(+) hematopoietic cell-based gene therapy with a modified FGF-2 increased endosteal/trabecular bone formation in mice. Mol Ther. 2007; 15:1881–1889. [PubMed: 17637718]
18. Meng X, Baylink DJ, Sheng M, Wang H, Gridley DS, Lau KH, et al. Erythroid promoter confines FGF2 expression to the marrow after hematopoietic stem cell gene therapy and leads to enhanced endosteal bone formation. PLoS One. 2012; 7:e37569. [PubMed: 22629419]
19. Hall SL, Chen ST, Gysin R, Gridley DS, Mohan S, Lau KH. Stem cell antigen-1+ cell-based bone morphogenetic protein-4 gene transfer strategy in mice failed to promote endosteal bone formation. J Gene Med. 2009; 11:877–888. [PubMed: 19629966]
20. Hall SL, Chen ST, Wergedal JE, Gridley DS, Mohan S, Lau KH. Stem cell antigen-1 positive cell-based systemic human growth hormone gene transfer strategy increases endosteal bone resorption and bone loss in mice. J Gene Med. 2011; 13:77–88. [PubMed: 21322098]
21. Pun S, Florio CL, Wronski TJ. Anabolic effects of basic fibroblast growth factor in the tibial diaphysis of ovariectomized rats. Bone. 2000; 27:197–202. [PubMed: 10913911]

22. Lane NE, Yao W, Kinney JH, Modin G, Balooch M, Wronski TJ. Both hPTH(1–34) and bFGF increase trabecular bone mass in osteopenic rats but they have different effects on trabecular bone architecture. J Bone Miner Res. 2003; 18:2105–2115. [PubMed: 14672345]
23. Nagai H, Tsukuda R, Mayahara H. Effects of basic fibroblast growth factor (bFGF) on bone formation in growing rats. Bone. 1995; 16:367–373. [PubMed: 7786640]
24. Aguirre JI, Leal ME, Rivera MF, Vanegas SM, Jorgensen M, Wronski TJ. Effects of basic fibroblast growth factor and a prostaglandin E2 receptor subtype 4 agonist on osteoblastogenesis and adipogenesis in aged ovariectomized rats. J Bone Miner Res. 2007; 22:877–888. [PubMed: 17352655]
25. Pun S, Dearden RL, Ratkus AM, Liang H, Wronski TJ. Decreased bone anabolic effect of basic fibroblast growth factor at fatty marrow sites in ovariectomized rats. Bone. 2001; 28:220–226. [PubMed: 11182382]
26. Tanaka Y, Inoue T. Fatty marrow in the vertebrae. A parameter for hematopoietic activity in the aged. J Gerontol. 1976; 31:527–532. [PubMed: 950446]
27. Pittenger MF, Mackay AM, Beck SC, Jaiswal RK, Douglas R, Mosca JD, et al. Multilineage potential of adult human mesenchymal stem cells. Science. 1999; 284:143–147. [PubMed: 10102814]
28. Xiao L, Sobue T, Esliger A, Kronenberg MS, Coffin JD, Doetschman T, et al. Disruption of the Fgf2 gene activates the adipogenic and suppresses the osteogenic program in mesenchymal marrow stromal stem cells. Bone. 2010; 47:360–370. [PubMed: 20510392]
29. Martin I, Muraglia A, Campanile G, Cancedda R, Quarto R. Fibroblast growth factor-2 supports ex vivo expansion and maintenance of osteogenic precursors from human bone marrow. Endocrinology. 1997; 138:4456–4462. [PubMed: 9322963]
30. Pitaru S, Kotev-Emeth S, Noff D, Kaffuler S, Savion N. Effect of basic fibroblast growth factor on the growth and differentiation of adult stromal bone marrow cells: enhanced development of mineralized bone-like tissue in culture. J Bone Miner Res. 1993; 8:919–929. [PubMed: 8213254]
31. Fei Y, Xiao L, Doetschman T, Coffin DJ, Hurley MM. Fibroblast growth factor 2 stimulation of osteoblast differentiation and bone formation is mediated by modulation of the Wnt signaling pathway. J Biol Chem. 2011; 286:40575–40583. [PubMed: 21987573]
32. Hurley MM, Lee SK, Raisz LG, Bernecker P, Lorenzo J. Basic fibroblast growth factor induces osteoclast formation in murine bone marrow cultures. Bone. 1998; 22:309–316. [PubMed: 9556129]
33. Okada Y, Montero A, Zhang X, Sobue T, Lorenzo J, Doetschman T, et al. Impaired osteoclast formation in bone marrow cultures of Fgf2 null mice in response to parathyroid hormone. J Biol Chem. 2003; 278:21258–21266. [PubMed: 12665515]
34. Kawaguchi H, Chikazu D, Nakamura K, Kumegawa M, Hakeda Y. Direct and indirect actions of fibroblast growth factor 2 on osteoclastic bone resorption in cultures. J Bone Miner Res. 2000; 15:466–473. [PubMed: 10750561]
35. Chikazu D, Hakeda Y, Ogata N, Nemoto K, Itabashi A, Takato T, et al. Fibroblast growth factor (FGF)-2 directly stimulates mature osteoclast function through activation of FGF receptor 1 and p42/p44 MAP kinase. J Biol Chem. 2000; 275:31444–31450. [PubMed: 10896947]
36. Zuo J, Jiang J, Dolce C, Holliday LS. Effects of basic fibroblast growth factor on osteoclasts and osteoclast-like cells. Biochem Biophys Res Commun. 2004; 318:162–167. [PubMed: 15110768]
37. During A, Penel G, Hardouin P. Understanding the local actions of lipids in bone physiology. Prog Lipid Res. 2015; 59:126–146. [PubMed: 26118851]
38. Nocka K, Tan JC, Chiu E, Chu TY, Ray P, Traktman P, et al. Molecular bases of dominant negative and loss of function mutations at the murine c-kit/white spotting locus: W37, Wv, W41 and W. EMBO J. 1990; 9:1805–1813. [PubMed: 1693331]
39. Geissler EN, Russell ES. Analysis of the hematopoietic effects of new dominant spotting (W) mutations of the mouse. Influence upon hematopoietic stem cells. Exp Hematol. 1983; 11:452–460. [PubMed: 6352297]
40. Trevisan M, Yan XQ, Iscove NN. Cycle initiation and colony formation in culture by murine marrow cells with long-term reconstituting potential in vivo. Blood. 1996; 88:4149–4158. [PubMed: 8943849]

41. Smith ER, Yeasky T, Wei JQ, Miki RA, Cai KQ, Smedberg JL, et al. White spotting variant mouse as an experimental model for ovarian aging and menopausal biology. Menopause. 2012; 19:588–596. [PubMed: 22228319]

42. Pachero RSH. Effects of radiation on bone. Curr Osteoporos Rep. 2013; 11:299–304. [PubMed: 24057133]

43. Chen ST, Gysin R, Kapur S, Baylink DJ, Lau KH. Modifications of the fibroblast growth factor-2 gene led to a marked enhancement in secretion and stability of the recombinant fibroblast growth factor-2 protein. J Cell Biochem. 2007; 100:1493–1508. [PubMed: 17243099]

44. Peng H, Chen ST, Wergedal JE, Polo JM, Yee JK, Lau KH, et al. Development of an MFG-based retroviral vector system for secretion of high levels of functionally active human BMP4. Mol Ther. 2001; 4:95–104. [PubMed: 11482980]

45. Livak KJ, Schmittgen TD. Analysis of relative gene expression data using real-time quantitative PCR and the 2(−Delta Delta C(T)) Method. Methods. 2001; 25:402–408. [PubMed: 11846609]

46. Farley JR, Hall SL, Herring S, Tarbaux NM. Two biochemical indices of mouse bone formation are increased, in vivo, in response to calcitonin. Calcif Tissue Int. 1992; 50:67–73. [PubMed: 1310883]

47. Sheng MH, Amoui M, Stiffel V, Srivastava AK, Wergedal JE, Lau KH. Targeted transgenic expression of an osteoclastic transmembrane protein-tyrosine phosphatase in cells of osteoclastic lineage increases bone resorption and bone loss in male young adult mice. J Biol Chem. 2009; 284:11531–11545. [PubMed: 19244239]

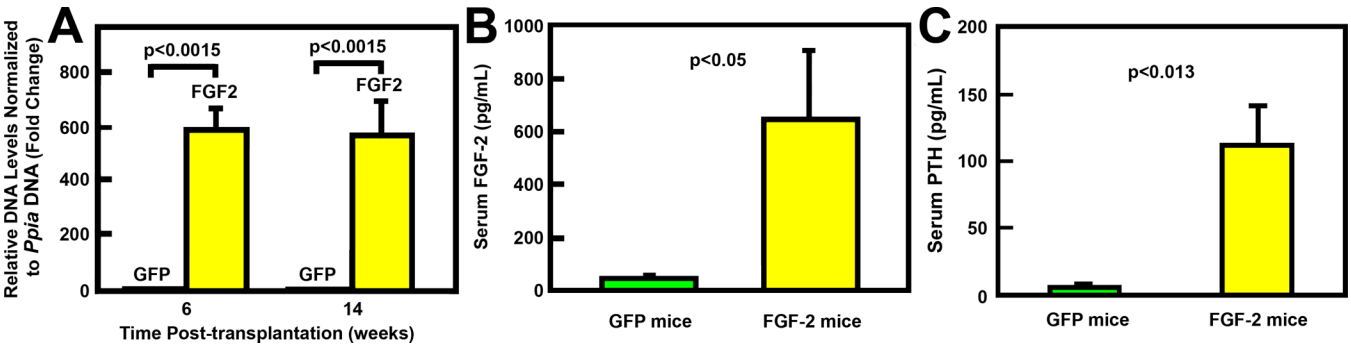

Figure 1.

Effects of marrow transplantation of MLV-*FGF2*- or MLV-*gfp*-transduced Sca-1$^+$ cells on relative levels of engraftment (A), as well as serum levels of FGF2 (B), and serum PTH (C) in recipient mice. In A, engraftment of FGF2-expressing Sca-1$^+$ cells was assessed by measuring the relative level of human *FGF2* genomic DNA content in peripheral blood cells of recipient mice of MLV-*FGF2*-transduced cells (FGF2) or control MLV-*gfp*-transduced cells (GFP) at 6 or 14 weeks post-transplantation, respectively. N = 7 per group. In B, serum FGF2 levels of recipient mice of MLV-FGF2-transduced cells (FGF-2 mice) or the control MLV-gfp-transduced cells (GFP mice) at 14 weeks post-transplantation were assayed with a commercial ELISA kit. N = 7 per group. In C, serum PTH levels of recipient mice of MLV-*FGF2*- or MLV-*gfp*-transduced Sca-1+ cells at 14 weeks post-transplantation were measured with a commercial ELISA kit. N = 7 per group.

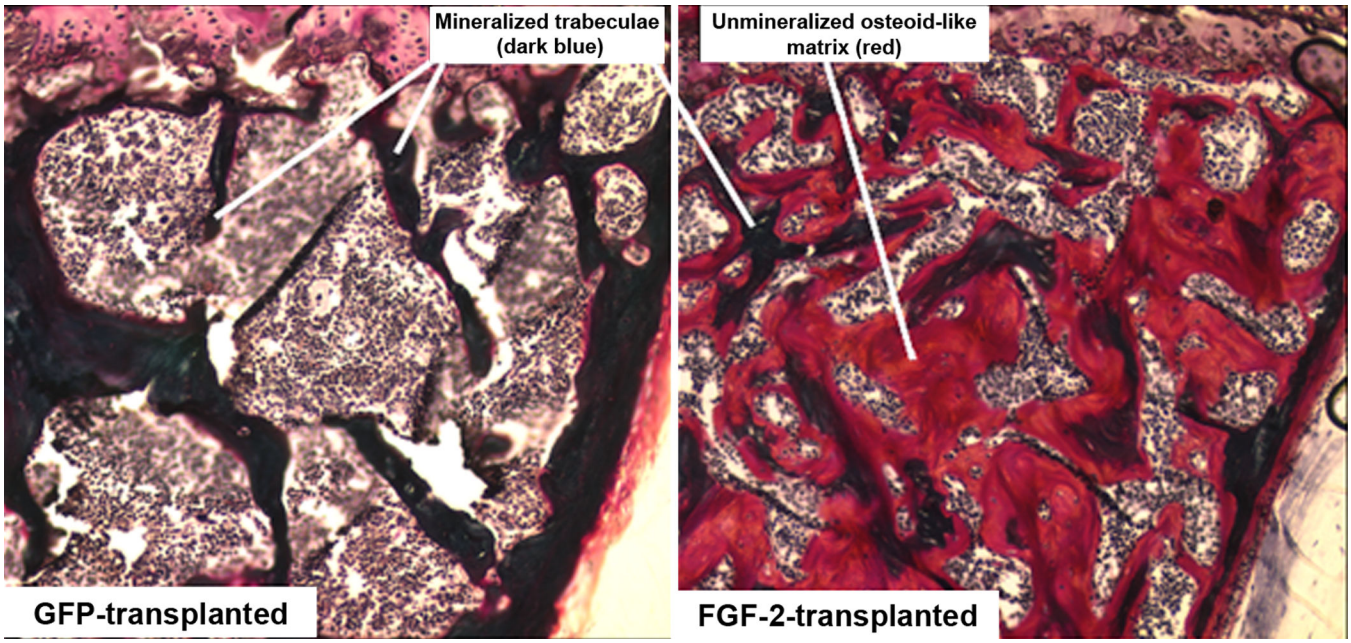

Figure 2.

Sca-1$^+$ cell-based systemic FGF2 gene therapy promoted massive trabecular bone formation but also caused osteomalacia in recipient mice. In A, a cross-sectional slice (5 μm in thickness) of L3 lumbar vertebrae of a representative control mice receiving the marrow transplantation of MLV-*gfp*-transduced Sca-1$^+$ cells at 14 weeks post-transplantation stained with the Goldner's trichrome dye for mineralized bone. In B, a cross-sectional slice (5 μm in thickness) of L3 lumbar vertebrae of a representative mice receiving the marrow transplantation of MLV-*FGF2*-transduced Sca-1$^+$ cells at 14 weeks post-transplantation stained with the Goldner's trichrome dye for mineralized bone. Mineralized bone is stained dark blue in color, whereas un-mineralized bone matrix is stained in red.

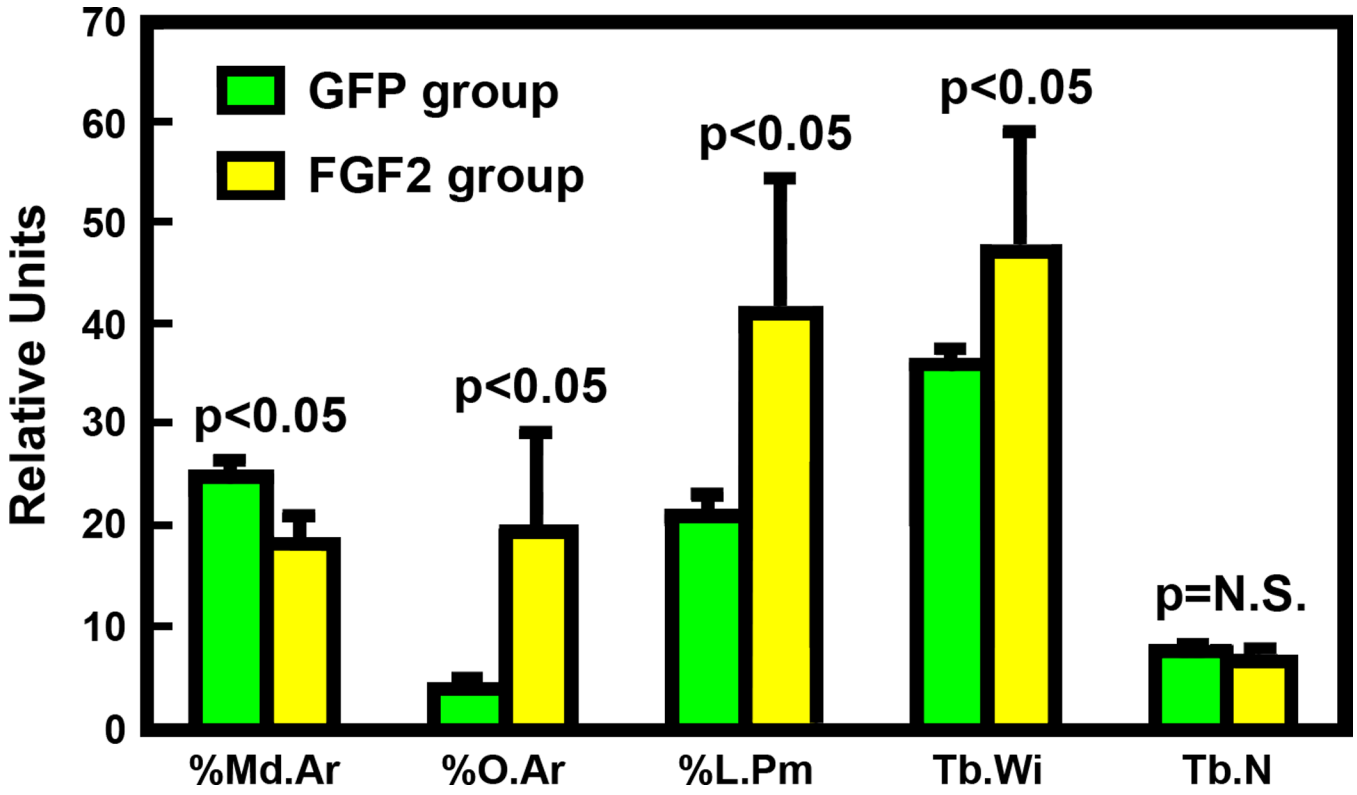

Figure 3.

Static bone histomorphometric parameters of L3 vertebrae of recipient mice of MLV-*gfp*-transduced Sca-1$^+$ cells (green bars) or MLV-*FGF2*-transduced Sca-1$^+$ cells (yellow bars) at 14 weeks post-transplantation. %Md.Ar, % mineralized bone area; %O.Ar, % osteoid area; %L.Pm, % bone forming surface; Tb.Wi, trabecular width; and Tb.N, trabecular number. N = 7 per group. N.S. = not significant.

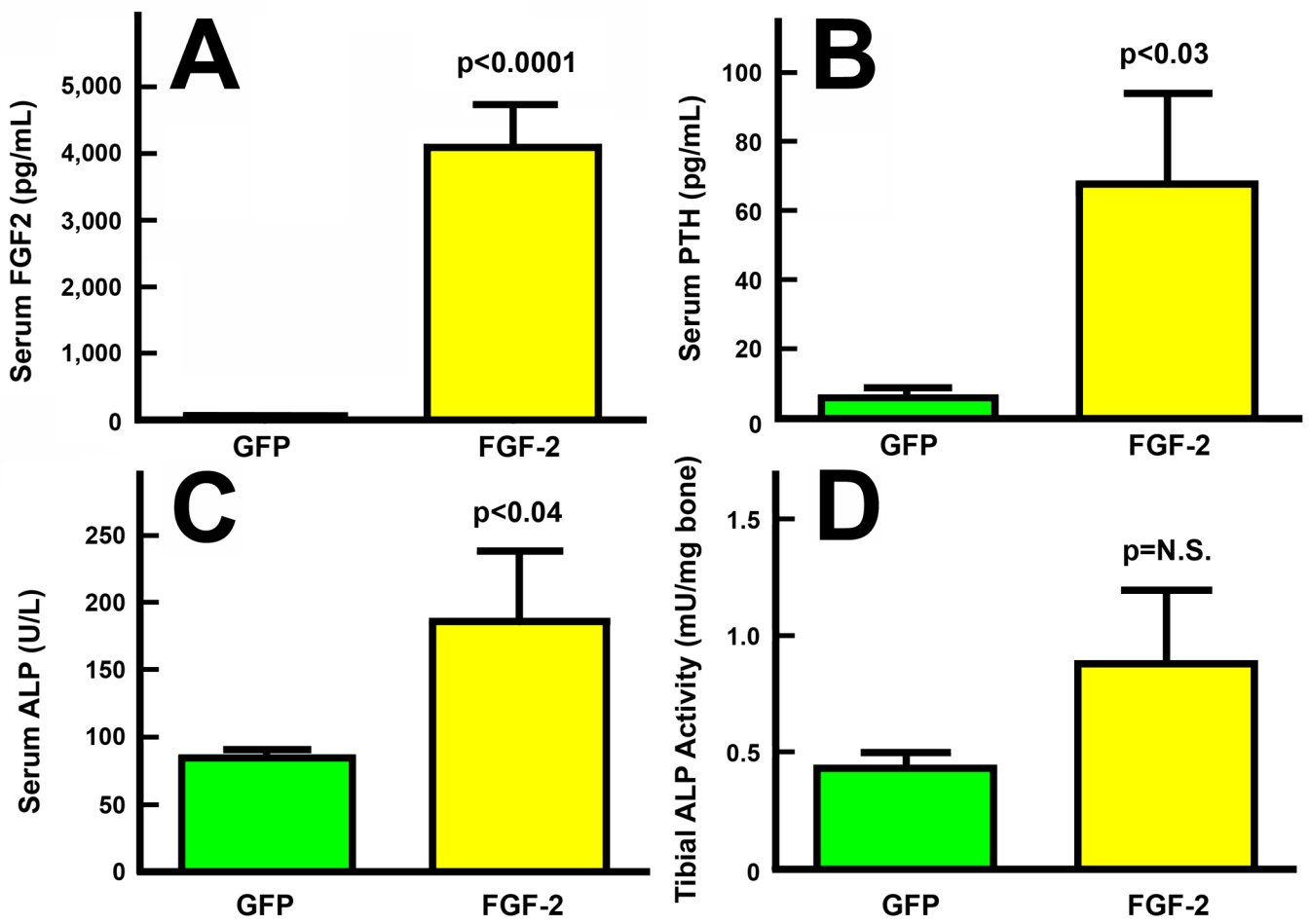

Figure 4.

Serum FGF2 (A), Serum PTH (B), Serum alkaline phosphatase (ALP) activity (C), and bone ALP activity (D) of recipient mice receiving either MLV-*FGF2*-transduced Sca-1$^+$ cells (FGF-2) or MLV-*gfp*-transduced Sca-1$^+$ cells (GFP) after 14 weeks post-transplantation in the second marrow transplantation experiment. FGF2 and PTH were measured with respective commercial ELISA kits. ALP activity was assayed as described in Materials and Methods. N = 7 for the GFP group, and N = 4 for the FGF2 group.

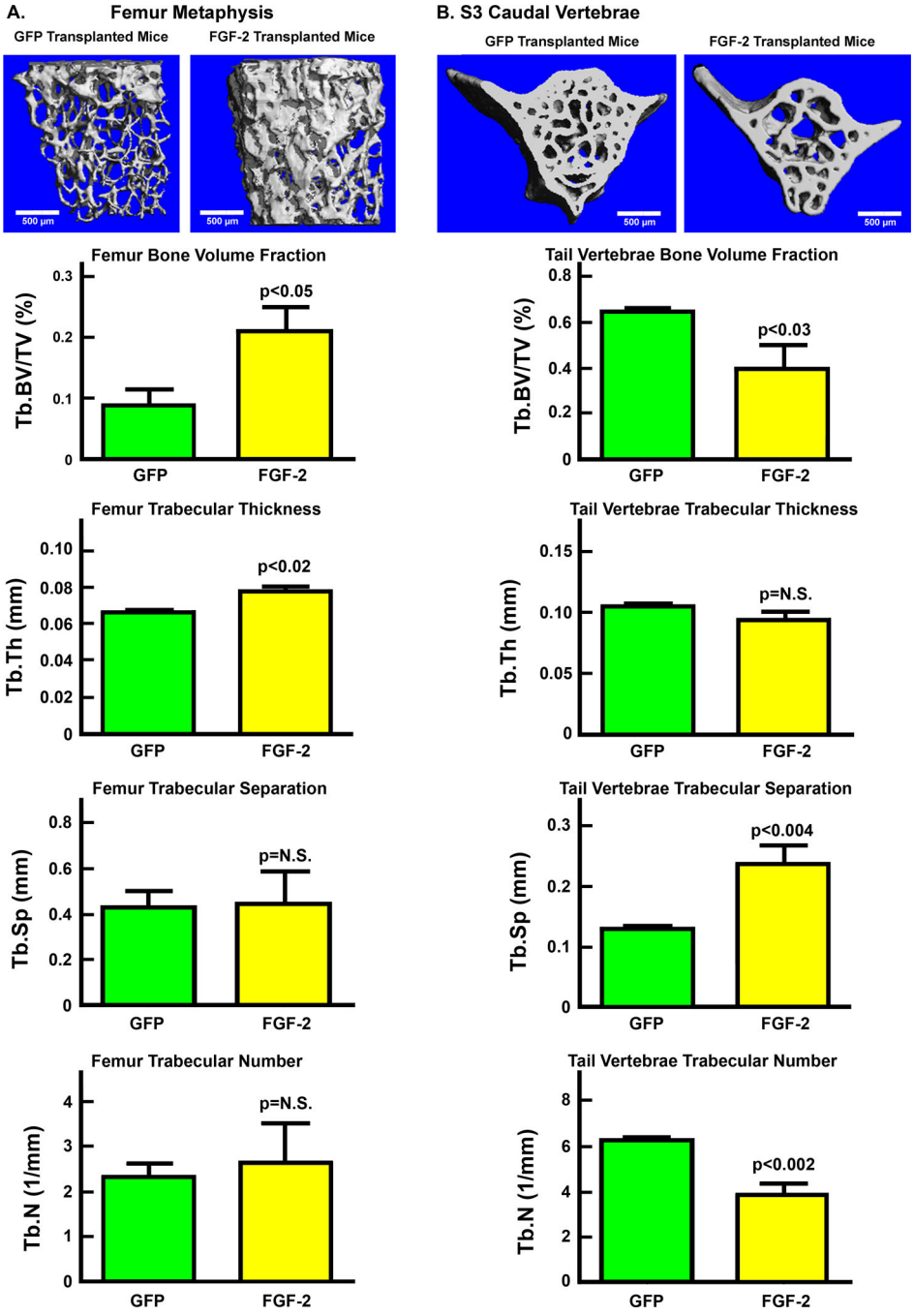

Figure 5.

Micro-CT analyses at the secondary spongiosa of the distal femur (A) or at S3 caudal vertebra (B) of recipient mice receiving either MLV-*FGF2*-transduced Sca-1$^+$ cells (FGF-2) or MLV-*gfp*-transduced Sca-1$^+$ cells (GFP) after 14 weeks post-transplantation. Top panels show a representative three-dimensional reconstruction of the trabecular structure each at the femur metaphysis (A) or at S3 caudal vertebrae (B) for each treatment group. Bottom bar graphs show the quantitative analyses of the three-dimensional bone parameters at each both site. N = 7 for the GFP group, and N = 4 for the FGF2 group.

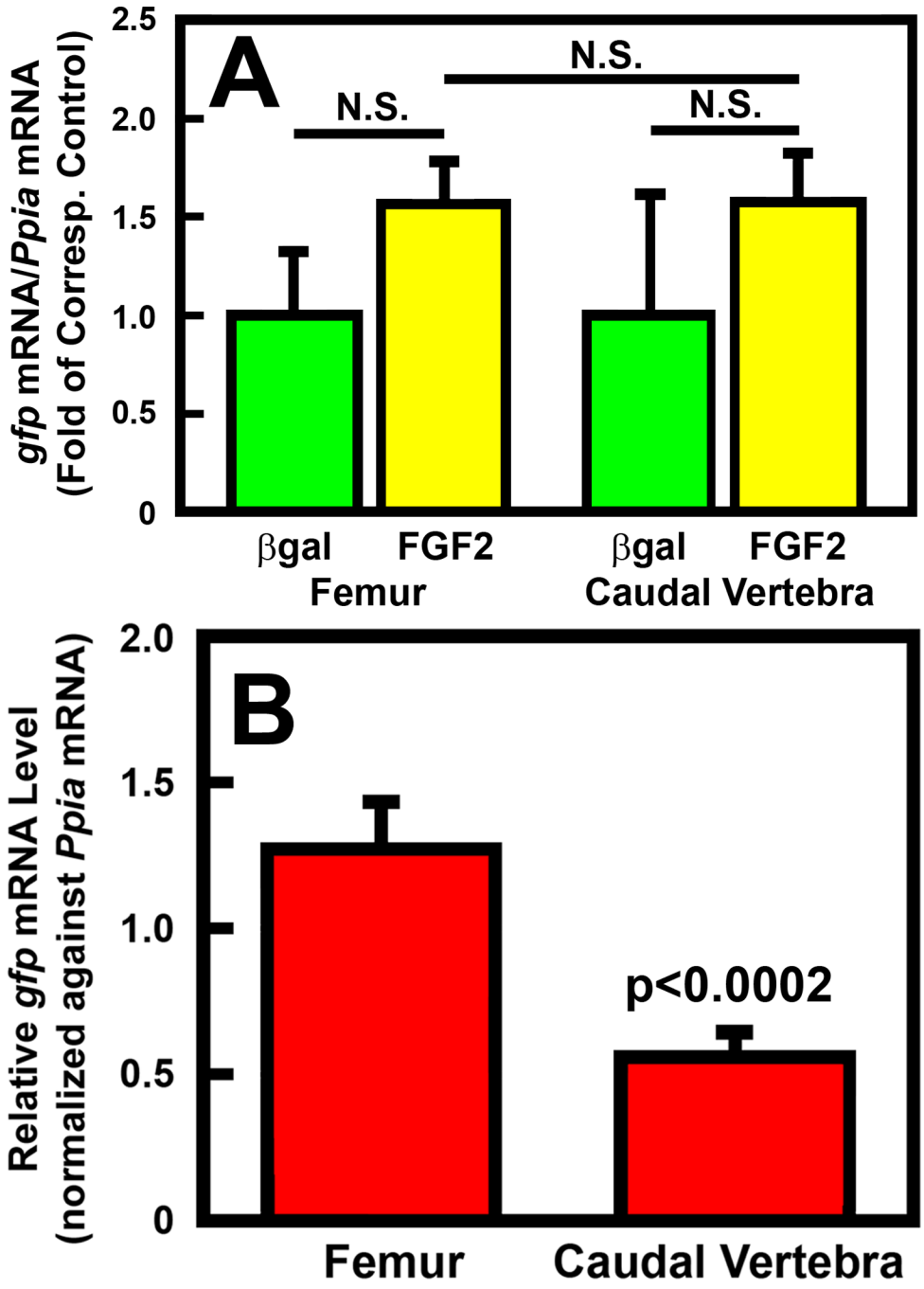

Figure 6.

A. Relative engraftment of transplanted β-galactosidase (βgal)-expressing cells at the marrow cavity of femurs (left columns) or at the entire caudal vertebra (right columns) of recipient mice receiving MLV-*FGF2*-transduced Sca-1$^+$ cells (FGF-2, N = 20) after 14 weeks post-transplantation compared to that of control recipient mice receiving MLV-*gfp*-transduced Sca-1$^+$ cells (GFP, N = 4). N.S. = not significant. B. Relative engraftment of *gfp*-expressing cells in the marrow cavity compared to that in the entire caudal vertebra of recipient mice receiving MLV-FGF2-transduced Sca-1$^+$ cells. N = 20 per group. Engraftment

in each panel was assessed by measuring the relative *gfp* mRNA levels (normalized against *Ppia* mRNA).

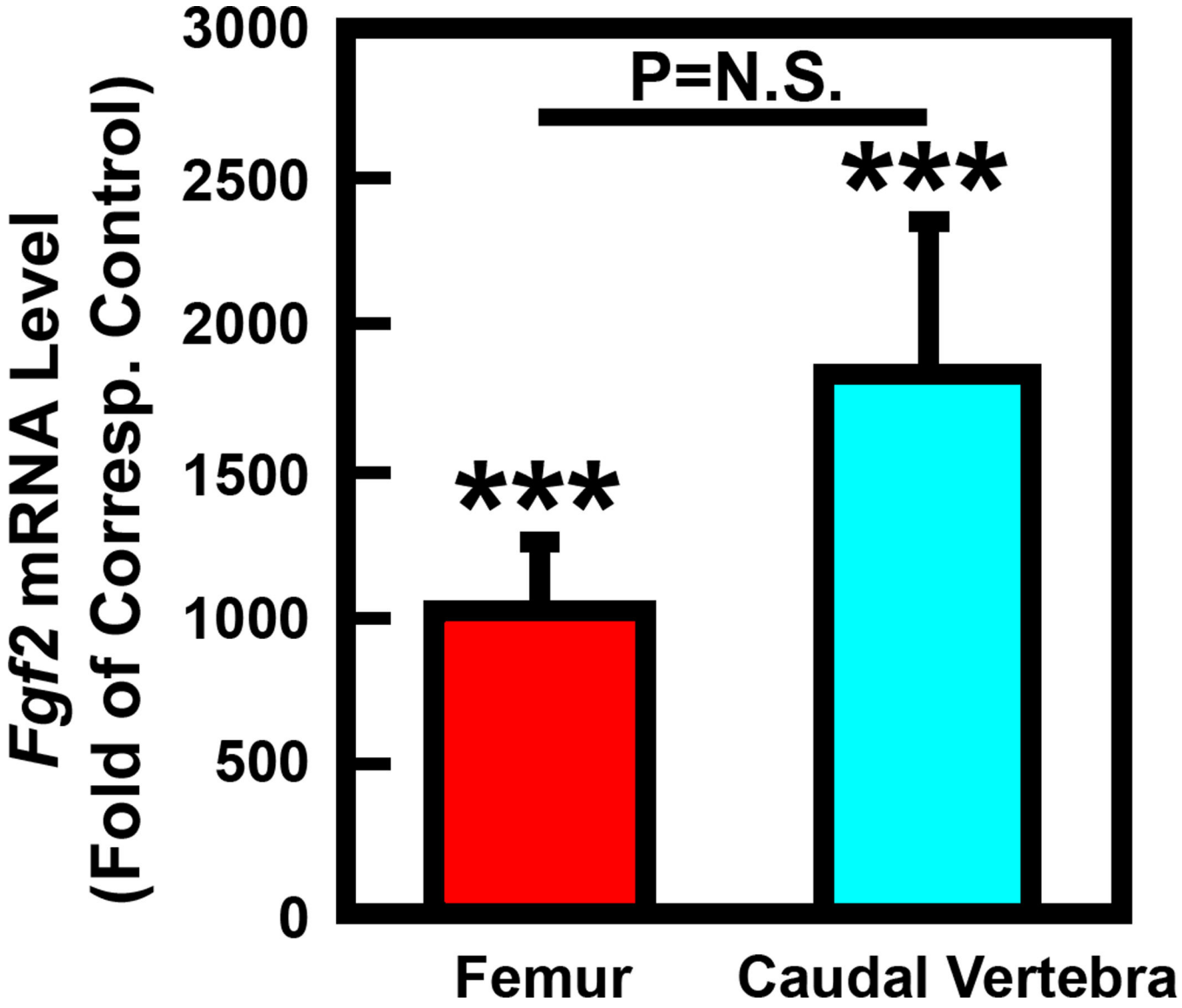

Figure 7.

Relative expression levels of *FGF2* mRNA in the marrow cavity or in the entire caudal vertebra of recipient mice receiving MLV-*FGF2*-transduced Sca-1$^+$ cells (N = 20) compared to respective *FGF2* mRNA expression levels at each bone site of control recipient mice receiving MLV-*gfp*-transduced cells (N = 4). *** P < 0.001 compared to respective GFP control group. N.S. = not significant.

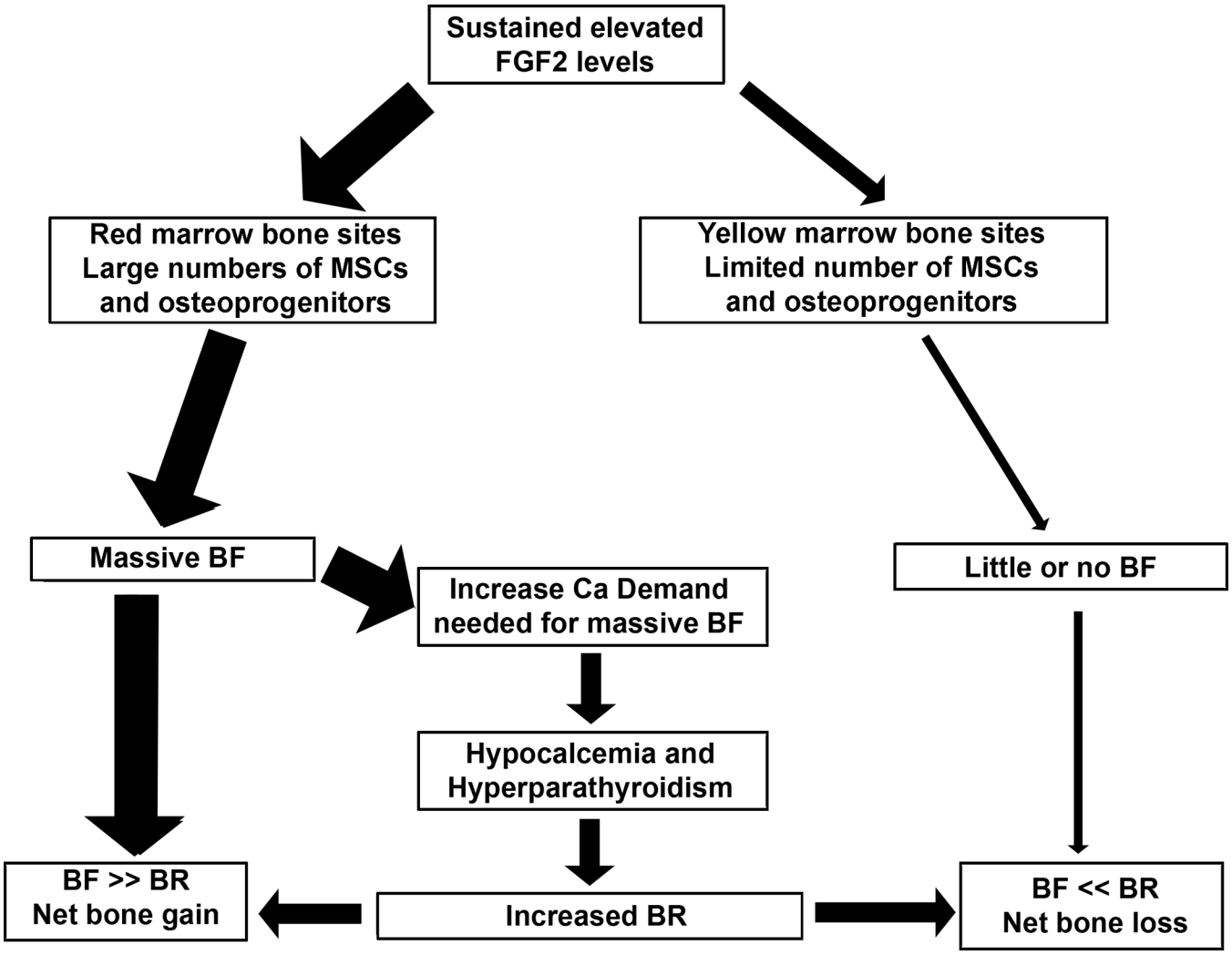

Figure 8.

A proposed model to account for the contrasting effects on the Sca-1^{+} cell-based systemic *FGF2* gene therapy on skeletal sites with red marrows as opposed to those on skeletal sites with yellow marrows. Please see text for detailed description of the model.